RESEARCH MEMORANDUM

INITIAL FLIGHT TESTS OF THE NACA FR-2, A HIGH-VELOCITY ROCKET-PROPELLED VEHICLE FOR TRANSONIC FLUTTER RESEARCH

By

J. G. Bamby and J. M. Teitelbaum

Langley Memorial Aeronautical Laboratory
Langley Field, Va.

NATIONAL ADVISORY COMMITTEE FOR AERONAUTICS

WASHINGTON

March 4, 1948

NATIONAL ADVISORY COMMITTEE FOR AERONAUTICS

RESEARCH MEMORANDUM

INITIAL FLIGHT TESTS OF THE NACA FR-2, A HIGH-VELOCITY ROCKET-PROPELLED VEHICLE FOR TRANSONIC FLUTTER RESEARCH

By J. G. Barmby and J. M. Teitelbaum

SUMMARY

The initial flight tests of two simplified flutter vehicles, which were launched at the Langley Pilotless Aircraft Research Station at Wallops Island, Va., are described herein.

The results of the tests are in agreement with the results of the freely-falling-body test in that the wing failures in the transonic range occurred at velocities greater than the flutter velocity calculated from the two-dimensional, incompressible theory.

Although the simple break-wire system seems satisfactory for exploratory tests, the scope of the investigation could be extended by use of a frequency-recording telemeter.

The use of high-velocity-rocket test vehicles of this type offers promise for flutter testing in the transonic and the supersonic regions.

INTRODUCTION

With present-day aircraft approaching sonic speeds, it becomes desirable to predict flutter conditions throughout the transonic and supersonic regions. This problem is being attacked by the National Advisory Committee for Aeronautics employing the Langley flutter tunnel, freely falling bodies, low-acceleration rocket-propelled vehicles, and high-velocity rocket-propelled vehicles. This last vehicle, designated the FR-2, is the only one capable of making flutter tests to a Mach number of 1.7 and was designed to be quickly and easily constructed and launched. The results of the initial flight tests of this vehicle are presented herein.

In order to check the stability of the model, the operation of the radio transmitter, and the ability of the trackers to obtain Doppler radar records over the desired range, models 1 and 2 were launched with only fins and instrumented nose. As these flights were successful, two sets

of flutter wings having similar characteristics were attached to models 3 and 4. The data obtained from the flights of models 3 and 4 are given in detail.

SYMBOLS

A	aspect ratio (including fuselage area)
M	Mach number
M_{cr}	theoretical Mach number at which sonic velocity is first attained on the airfoil at zero lift (reference 1)
c.g.	distance of center of gravity behind leading edge, percent chord
e.a.	distance of the elastic axis behind leading edge, percent chord
b	semichord of test wing, feet (reference 2)
a	nondimensional elastic axis position $\left(\frac{2e.a.}{100} - 1\right)$ (reference 2)
$a + x_\alpha$	nondimensional center-of-gravity position $\left(\frac{2c.g.}{100} - 1\right)$ (reference 2)
T	free-air temperature, $^\circ F$ absolute
p_s	static pressure, pounds per square foot
ρ	air density, pounds-second^2-feet^{-4}
κ	weight ratio $\left(\frac{\pi\rho b^2}{m}\right.$ where m is mass of airfoil per unit length$\left.\right)$
r_α^2	square of nondimensional radius of gyration about elastic axis $\left(\frac{I_\alpha}{mb^2}\right.$ where I_α is polar moment of inertia about elastic axis$\left.\right)$ (reference 2)
f_{h_1}	first bending natural frequency, cycles per second
f_{h_2}	second bending natural frequency, cycles per second

f_t first torsion natural frequency, cycles per second

f_α uncoupled torsion frequency about the elastic axis,

$$\text{cycles per second} \quad \left(f_t \left[1 - \frac{\left(\frac{x_\alpha}{r_\alpha}\right)^2}{1 - \left(\frac{f_{h_1}}{f_t}\right)^2} \right]^{1/2} \right)$$

ω_α uncoupled angular torsional frequency about the elastic axis, radians per second $(2\pi f_\alpha)$

V velocity, miles per hour

v velocity, feet per second

q dynamic pressure, pounds per square foot

t time after firing, seconds

$1g$ acceleration 32.2 feet per second per second

$\frac{v}{b\omega_\alpha}$ nondimensional flutter speed coefficient (reference 2)

V_{f_o} theoretical flutter velocity, miles per hour (two-dimensional incompressible theory employing first bending-torsion mode and density at time of failure $\left(\frac{60}{88}\frac{v}{b\omega_\alpha}\omega_\alpha b\right)$) (reference 2)

V_D theoretical divergence velocity, miles per hour (two-dimensional incompressible theory using density at time of failure) (reference 2)

APPARATUS

Model

The FR-2 models 3 and 4 were essentially standard 5-inch high-velocity aircraft rockets to which instrumented noses and flutter wings, identical for both models, had been added, resulting in a configuration which resembles conventional aircraft designs. The rocket motor

weighed 88.7 pounds, including 24.9 pounds of powder, and produced a thrust of 5000 pounds for approximately 1 second. In order to reduce the acceleration of the model so that trackers could obtain radar records through the desired velocity range, sufficient lead was added in the nose to increase the model weight to 112.5 pounds. A sketch of the model is shown in figure 1 and photographs of the model on the 60° launching rack are shown as figures 2(a) and 2(b).

Flutter Wings

The flutter wings, located slightly behind the center of gravity of the complete model, are shown in figure 3 and had the following characteristics:

Weight, pounds per wing	1.78
Area (including fuselage), square feet	2.77
Wing loading, pounds per square foot	40.7
A	6.8
Section	NACA 16-010
M_{cr}	0.80
c.g.	46.4
e.a.	31
b	1/3
a	-0.38
$a + x_\alpha$	-0.07
$(1/\kappa)$ standard density	34.1
r_α^2	0.363
f_{h_1}	23.7
f_{h_2}	136
f_t	125
f_α	107
f_{h_1}/f_α	0.22

Instrumentation

Each model was equipped with a radio transmitter housed in a Plexiglas nose. This transmitter provided a continuous-wave unmodulated radio frequency field which was approximately plane polarized in a plane normal to the plane of the transmitting antenna and of nearly circular-field-strength pattern. The positive battery lead of the power supply to the transmitter was fed from the battery through break wires in the flutter wings before supplying current to the plate of the transmitter. Wing failure, therefore, cut the power supply and stopped the transmitter from operating. A rotating antenna on the ground was polarization sensitive and a low-frequency signal due to the rotation of the antenna was produced at the output of the receiver. This signal was recorded as an oscillating wave on a film-type recorder as long as the transmitter in the model was operating. When the transmitter ceased to operate, the oscillation of the signal stopped. A part of the record is shown in figure 4. The flights of the models were tracked with Doppler radar in order that a velocity record could be obtained. Timing signals were simultaneously fed to both the Doppler radar and the radio-transmitter recorder in order that the data could be correlated.

RESULTS AND DISCUSSION

The flights of the models with wings were smooth prior to wing failure. The time histories of the model flights are shown in figures 5(a) and 5(b), in which flight velocities and Mach number are plotted as functions of time. From these curves the longitudinal accelerations were calculated for models 3 and 4, respectively, at time of wing failure. Figures 6(a) and 6(b) are photographs of the recovered wings. Wing failures occurred at a Mach number of 0.88 in each case. Conditions at the time of wing failure were as follows:

Parameter	Model 3	Model 4
M	0.88	0.88
V	675	675
p_s	2110	2110
T	522.2	522.2
ρ	0.00237	0.00237
q	1155	1155
$1/\kappa$	34.2	34.2
t	0.64	0.62
Acceleration.	52.0g	52.5g

A preliminary analysis of the test wings was made using two-dimensional incompressible theory. The theoretical divergence velocity V_D was 1098 miles per hour. The flutter velocity coefficient $v/b\omega_\alpha$ for the bending-torsion case of flutter was calculated for various frequency ratios f_h/f_α, as shown in figure 7. The first bending-frequency ratio f_{h_1}/f_α was used to determine the flutter coefficient of this wing. The value of V_{f_o} obtained was 528 miles per hour from two-dimensional incompressible flow theory. The results of the tests conducted show wing failure occurred at approximately 675 miles per hour for both models. It is seen that this experimental value obtained at a Mach number of 0.88 was 28 percent greater than that obtained using the two-dimensional, incompressible theoretical value. This basic flutter theory which does not consider the effects of aspect ratio, compressibility, and flutter-deflection pattern is used primarily as a standard to correlate the results with the other test methods.

Using as a basis of comparison the ratio of the experimental-failure velocity to the theoretical-flutter velocity, the results of these tests show agreement within a few percent with the results of the freely-falling-body test (reference 3). The low-acceleration freely falling body similarly employed a break-wire system.

Although the data compare favorably with the freely-falling-body test, the scope of the investigation could be extended by the use of a frequency-recording telemeter. From the telemeter record it would be possible to obtain data on the mode of flutter and any possible longitudinal acceleration effect on the variation in time interval between the start of flutter oscillations and wing failure.

CONCLUSIONS

1. The results of the tests are in agreement with the results of the freely-falling-body test in that the wing failures in the transonic range occurred at velocities greater than the flutter velocity calculated from the two-dimensional, incompressible theory.

2. Although the simple break-wire system seems satisfactory for exploratory tests, the scope of the investigation could be extended by use of a frequency-recording telemeter.

3. High-velocity aircraft rockets of this type offer promise as vehicles for flutter testing in the transonic and the supersonic regions.

Langley Memorial Aeronautical Laboratory
National Advisory Committee for Aeronautics
Langley Field, Va.

REFERENCES

1. Abbott, Ira H., von Doenhoff, Albert E., and Stivers, Louis S., Jr.: Summary of Airfoil Data. NACA ACR No. L5C05, 1945.

2. Theodorsen, Theodore, and Garrick, I. E.: Mechanism of Flutter - A Theoretical and Experimental Investigation of the Flutter Problem. NACA Rep. No. 685, 1940.

3. Barmby, J. G., and Clevenson, S. A.: Initial Test in the Transonic Range of Four Flutter Airfoils Attached to a Freely Falling Body. NACA RM No. L7B27, 1947.

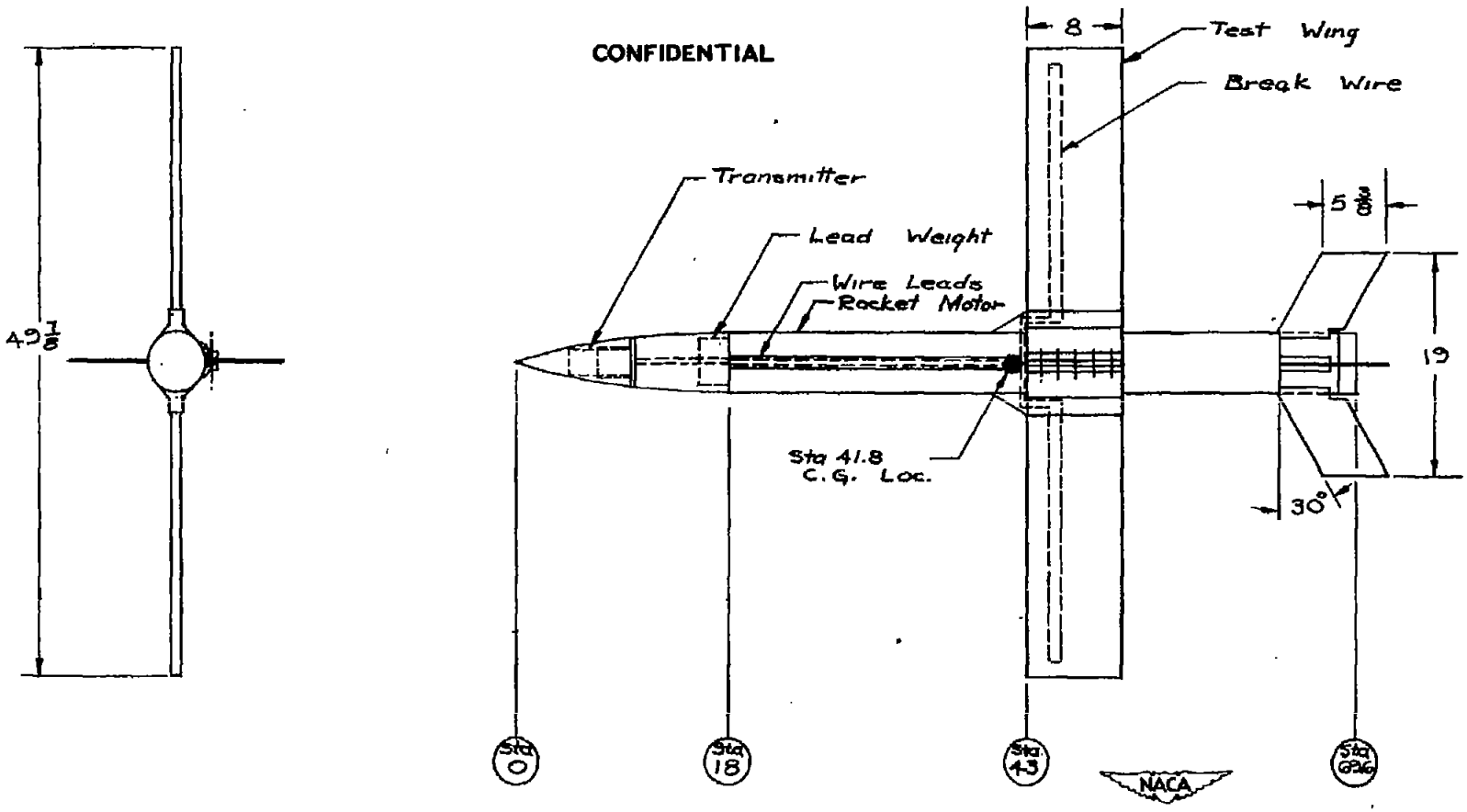

Figure 1.- Sketch of FR-2 models 3 and 4. (All dimensions are in inches.)

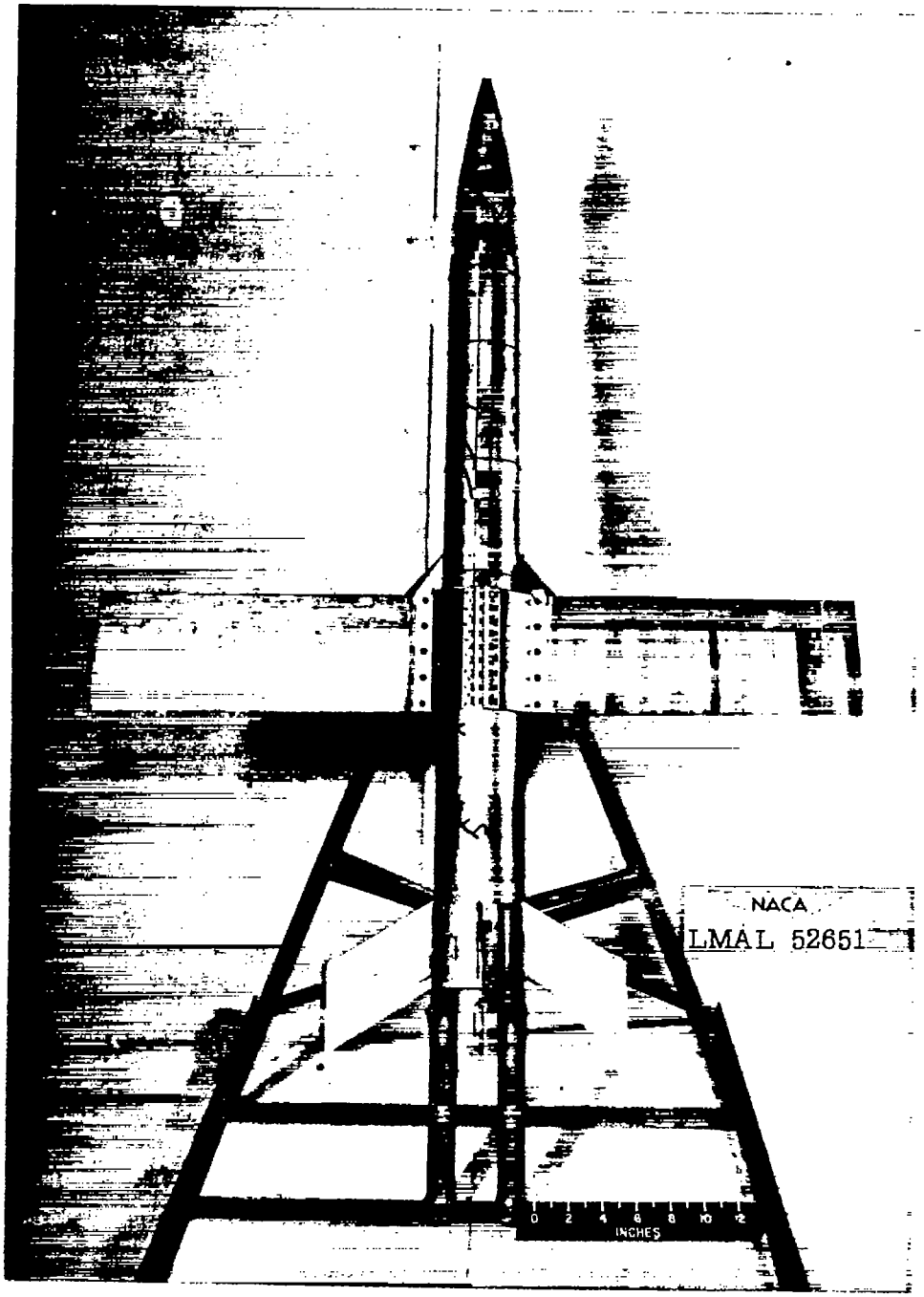

(a) Front view.

Figure 2.- Photograph of FR-2 model 3 on launching rack.

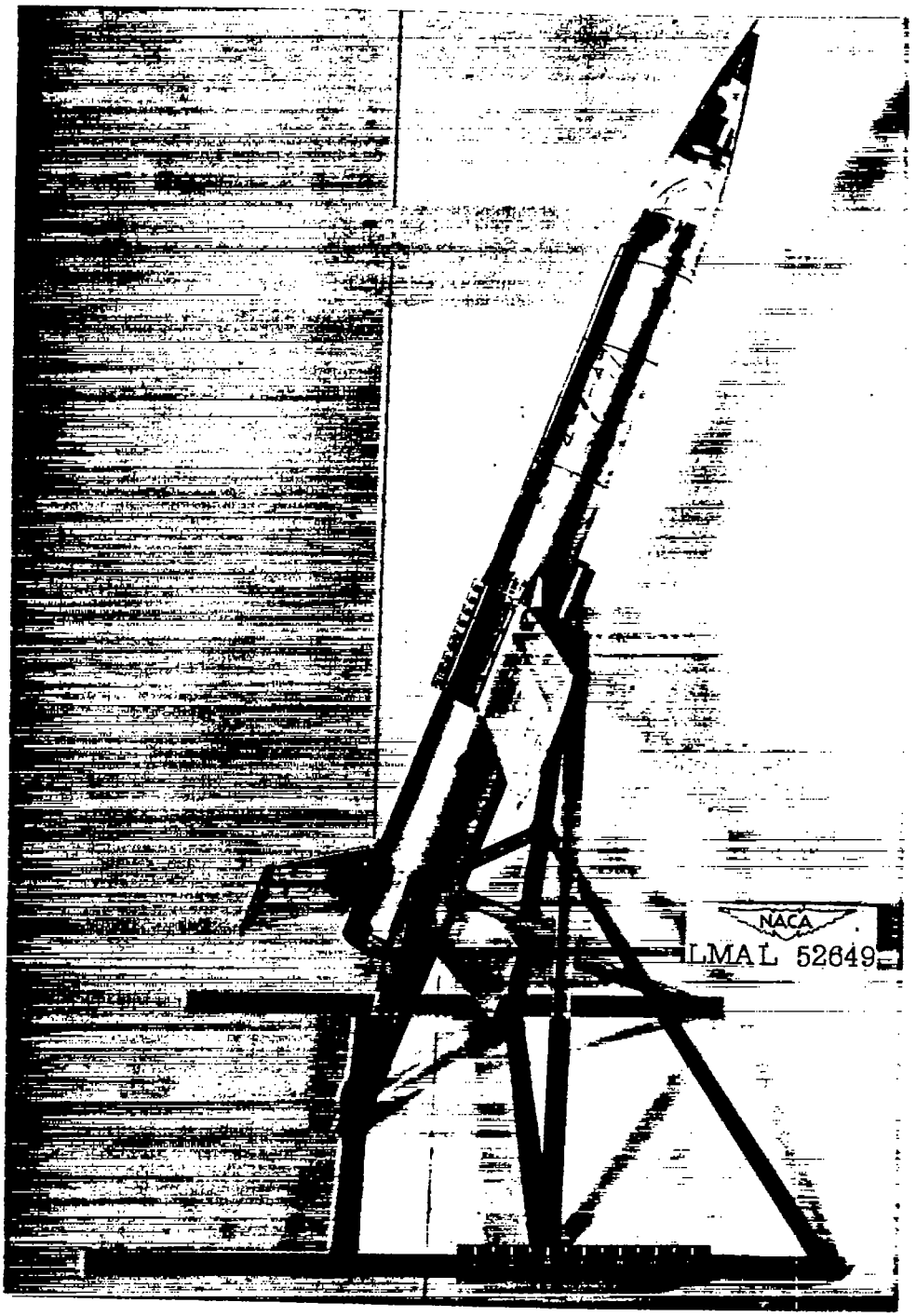

(b) Side view.

Figure 2.- Concluded.

CONFIDENTIAL

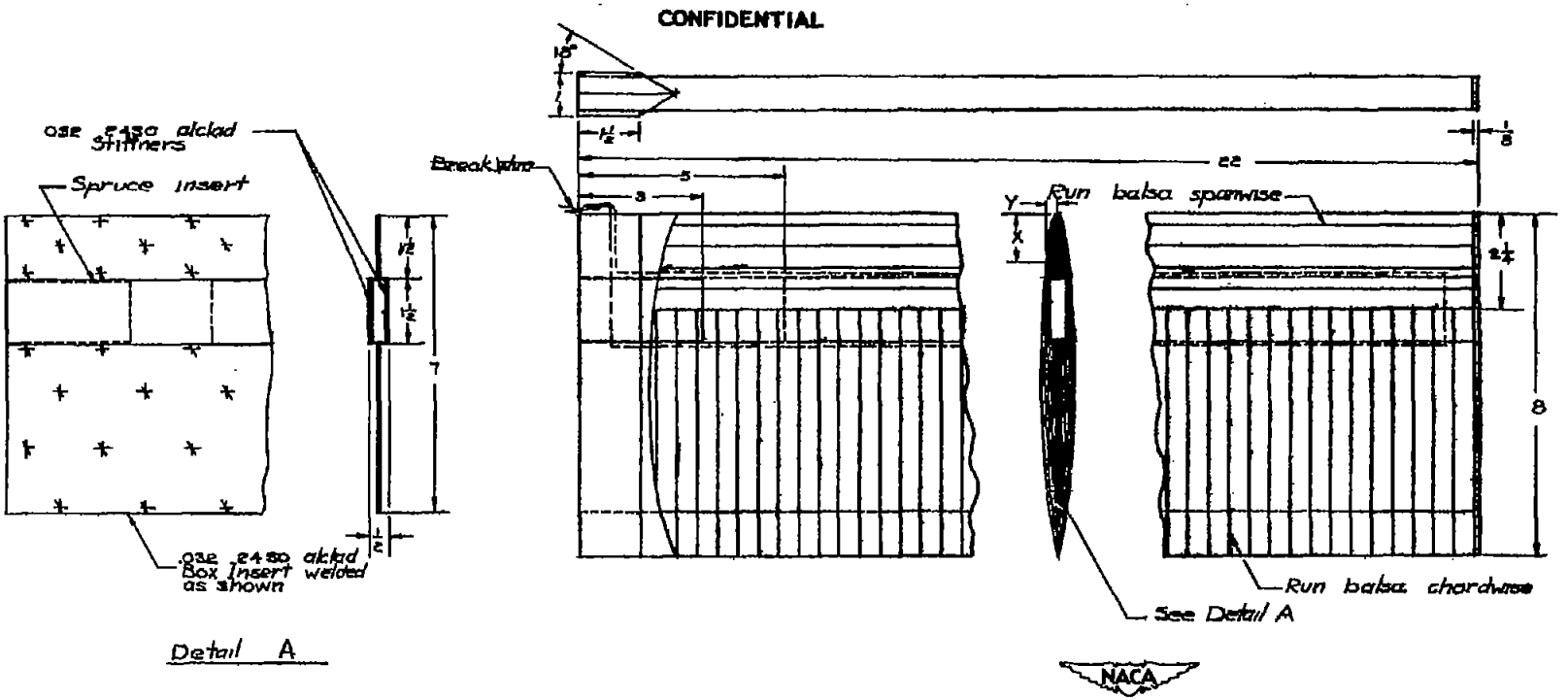

NACA 16-010 Airfoil Coordinates			
X	$Y_U = Y_L$	X	Y_U Y_L
0	0	2.400	.360
.100	.086	4.000	.400
.200	.120	5.600	.350
.400	.166	6.400	.280
.600	.202	7.200	.168
1.200	.276	7.600	.094
1.600	.310	8.000	.008
L. E. R. = .035 ±.005			

CONFIDENTIAL

Figure 3.- Sketch of flutter-test wings. (All dimensions are in inches.)

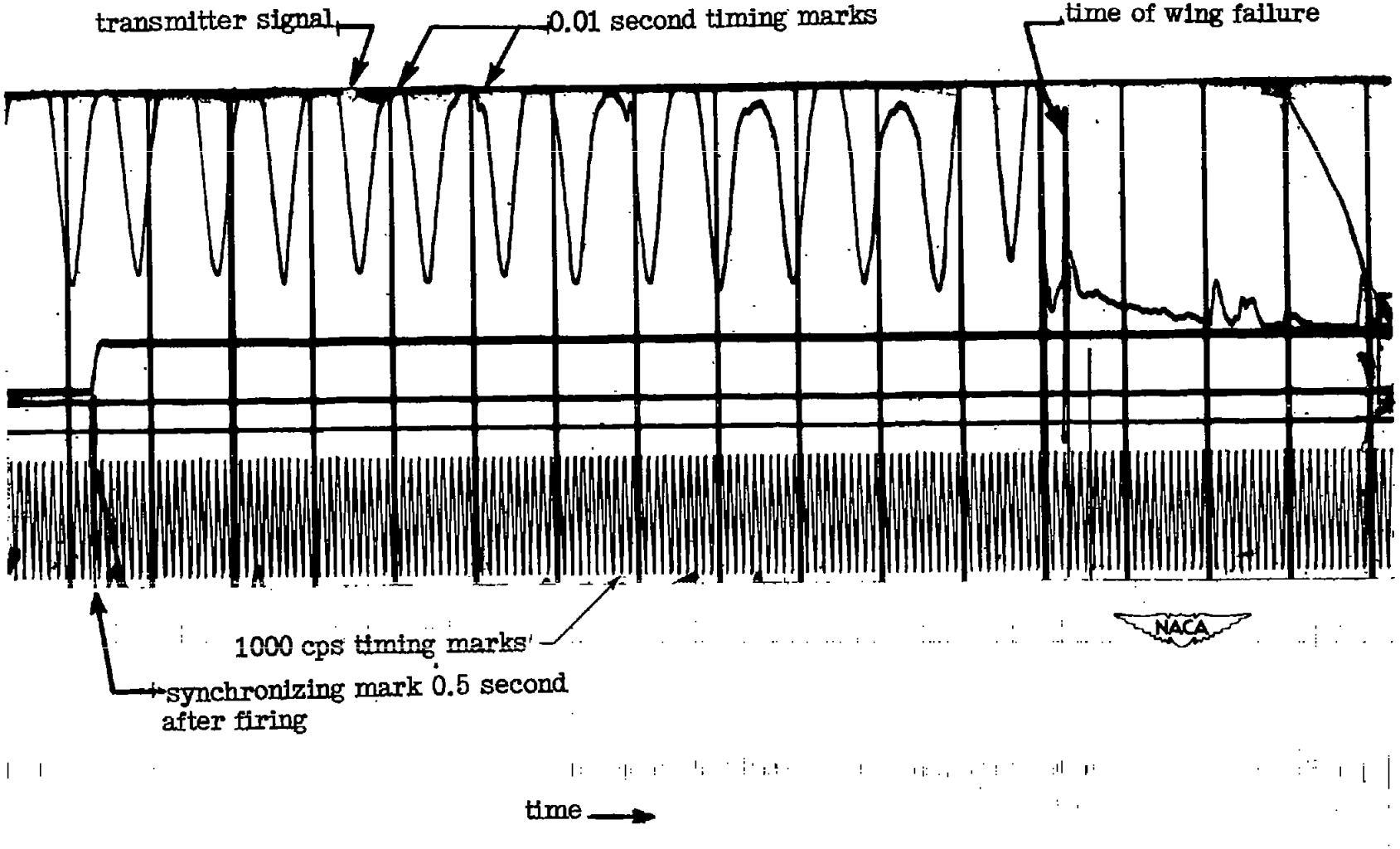

Figure 4.- Portion of radio transmitter record showing time of wing failure for the flight of the FR-2, model 4.

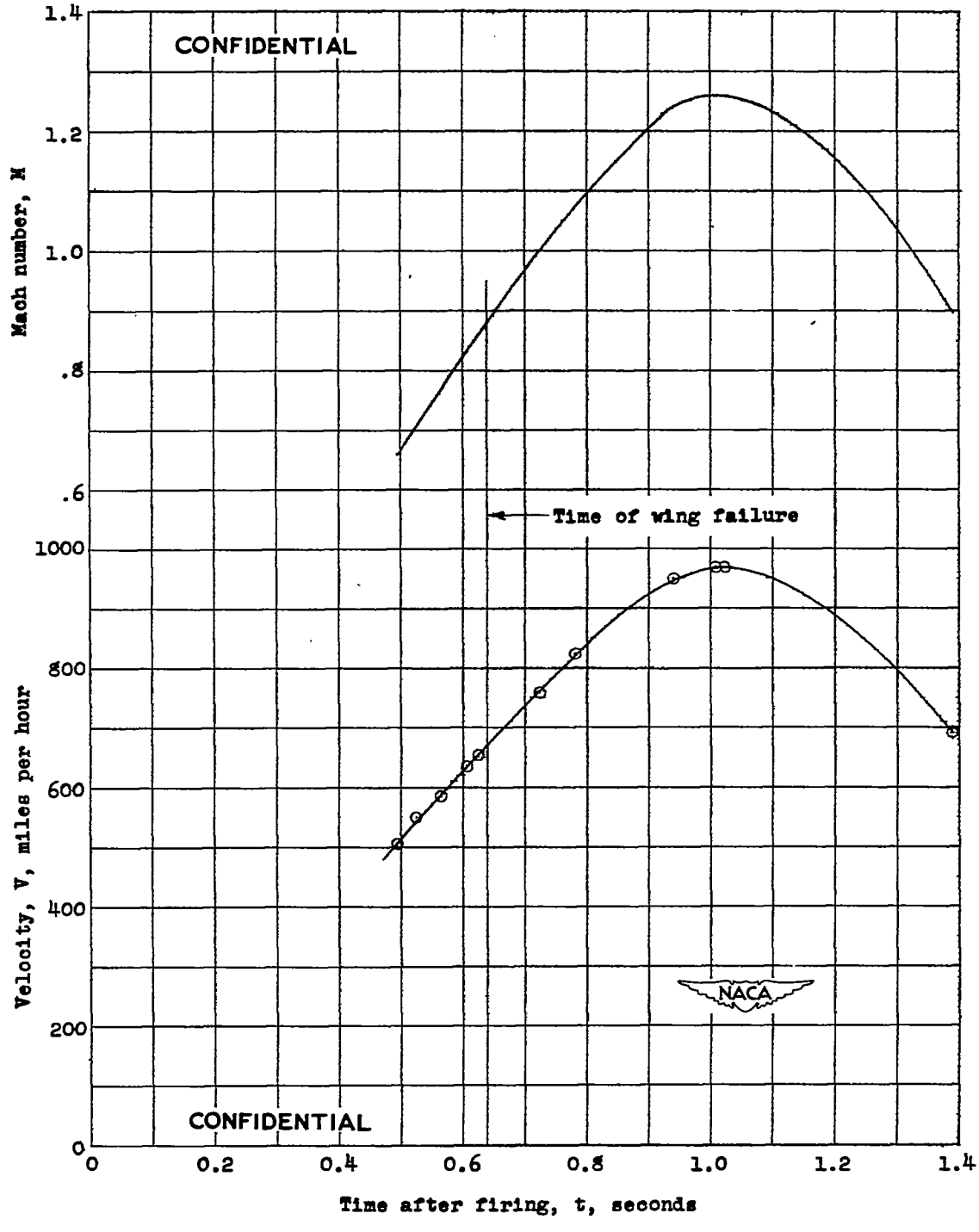

(a) Model 3.

Figure 5.- Time history of FR-2 in flight.

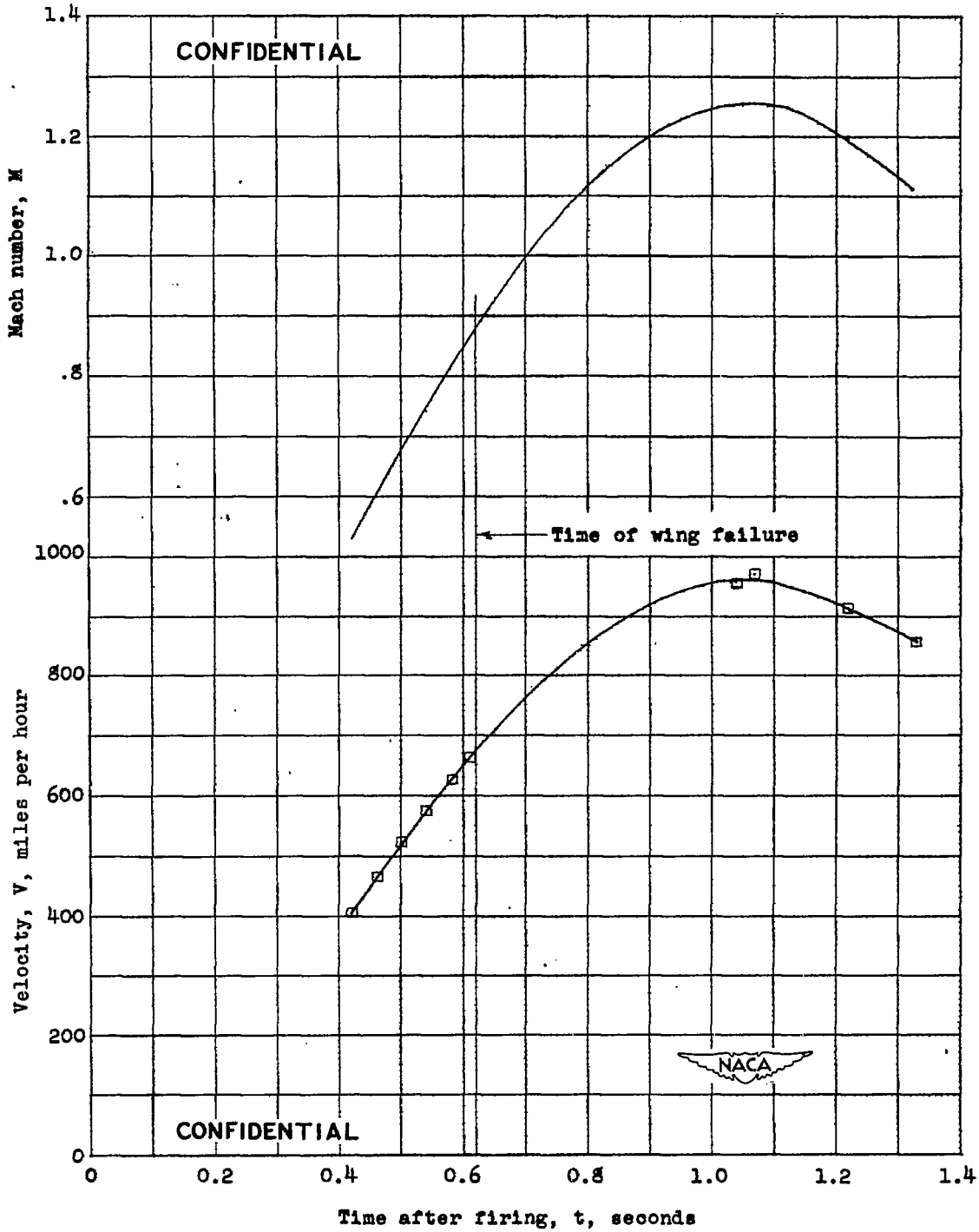

(b) Model 4.

Figure 5.- Concluded.

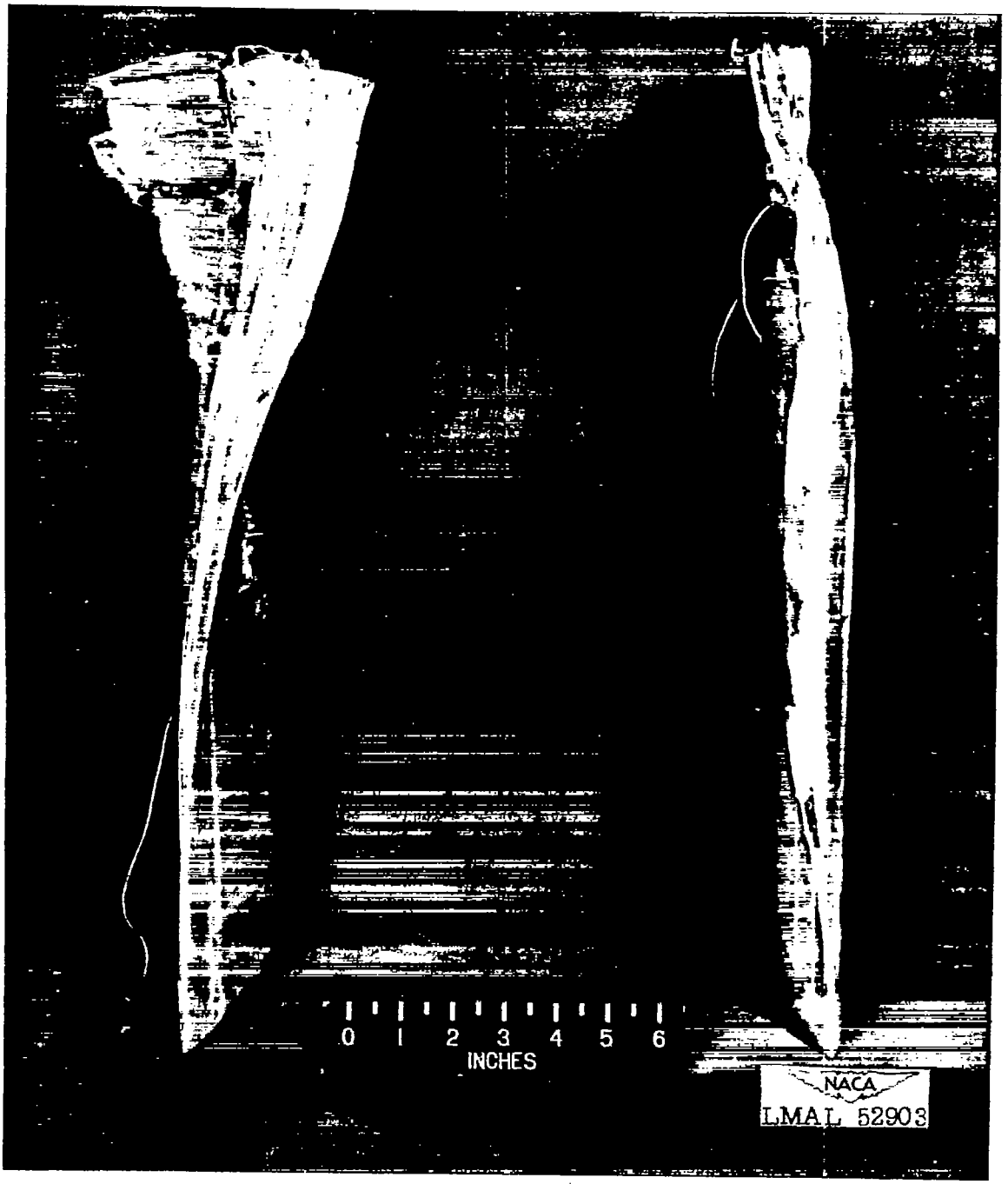

(a) Model 3.

Figure 6.- Photograph of test wings recovered from flight of FR-2.

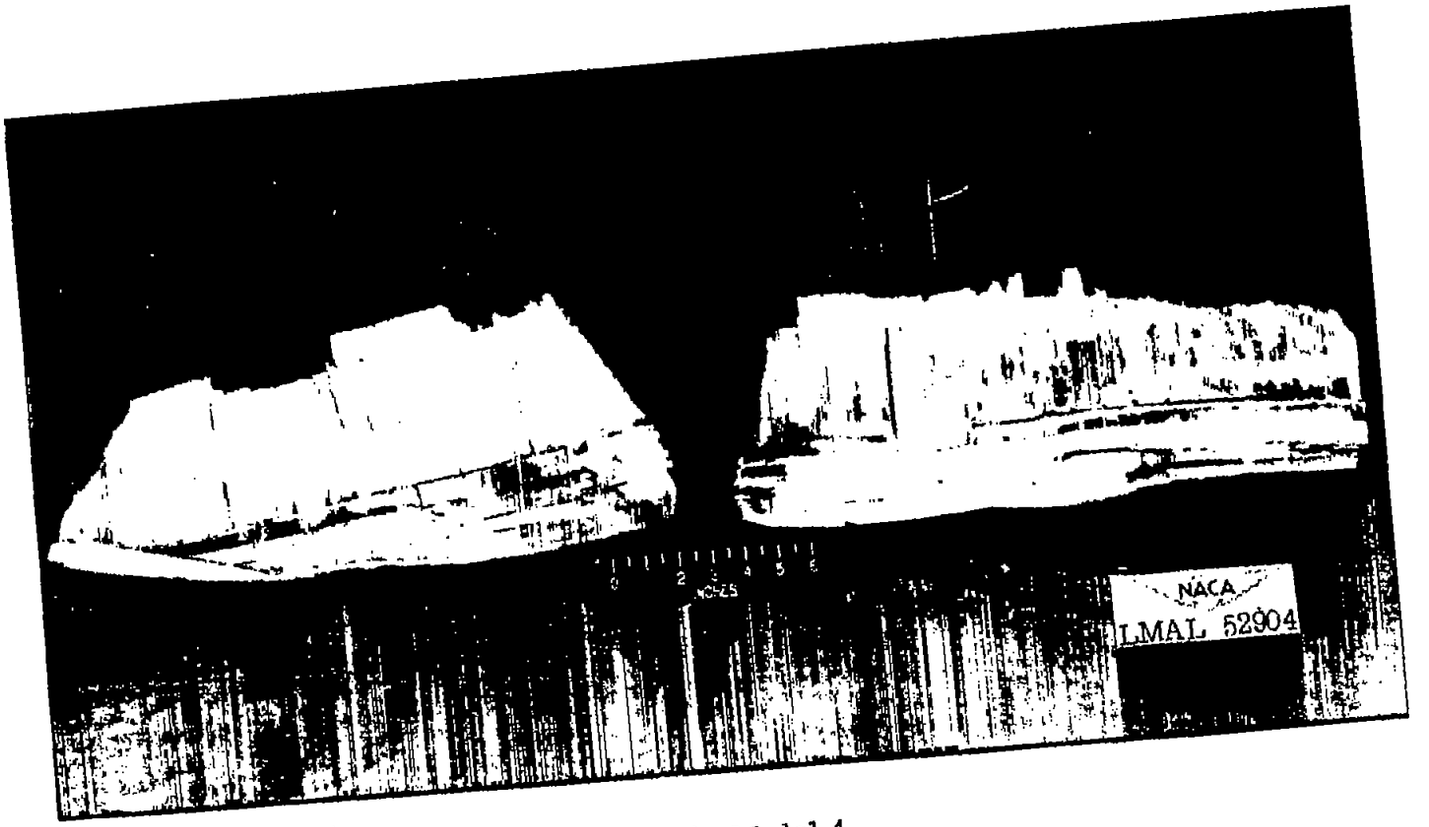

(b) Model 4.

Figure 6.- Concluded.

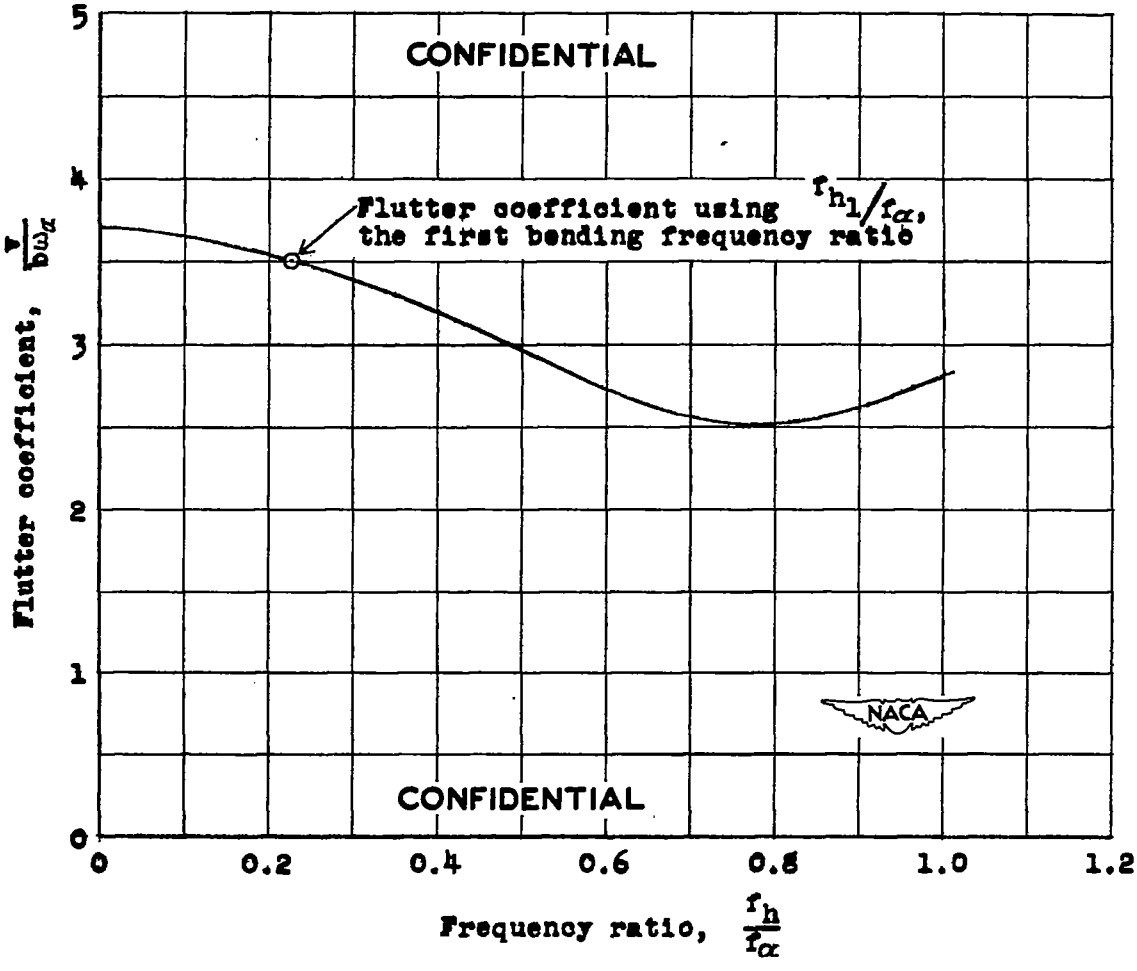

Figure 7.- Calculated flutter coefficient using first bending mode; two-dimensional, incompressible theory.